On the mathematical basis of solid friction

Mike R. Jeffrey

April 27, 2015

Abstract A piecewise-smooth ordinary differential equation model of a dry-friction oscillator is studied, as a paradigm for the role of nonlinear and hysteretic terms in discontinuities of dynamical systems. The friction discontinuity is a switch in direction of the contact force in the transition between left and rightward slipping motion. Nonlinear terms introduce dynamics that is novel in the context of piecewise-smooth dynamical systems theory (in particular they are outside the standard *Filippov* convention), but are shown to account naturally for static friction, and moreover provide a simple route to including hysteresis. The nonlinear terms are understood in terms of dummy dynamics at the discontinuity, given a formal derivation here. The result is a three-parameter model built on the minimal mathematical features necessary to account for the key characteristics of dry friction. The effect of compliance can be distinguished from the contact model, and numerical simulations reveal that all behaviours persist under smoothing and under small random perturbations, but nonlinear effects can be made to disappear abruptly amid sufficient noise.

1 Smooth or nonsmooth, regular or singular?

Different physical and mathematical approaches have provided an increasingly complex picture of the dynamics involved in friction, the contact force that arises along the interface between two solid bodies. In the light of developments in nonlinear and nonsmooth dynamics, in particular in the field of piecewise smooth dynamical systems, it is interesting to revisit the mathematical description of a phenomenon that seems fundamental to physical interaction.

Whereas Amontons and Coulomb wrote the now classical friction laws that give a coefficient μ relating the resistance force F to the normal load N as

$$F = \mu N \, ,$$

it has been proposed (see e.g. [17,51]) to add an adhesive contribution Na,

$$F = \mu(N + Na) \, .$$

Engineering Mathematics, University of Bristol, UK, email: mike.jeffrey@bristol.ac.uk

There are of course many ways to go about this by different physical arguments. The purpose of this paper is to obtain a simple form for such a term by mathematical principles alone, and study its consequences using recent ideas from piecewise smooth dynamical systems theory.

We should emphasise from the outset that this paper is not intended to propose an ultimate friction model, rather it is intended to take certain behaviours discovered in the theoretical study of piecewise-smooth dynamical systems, and gain insight into their possible role in a well-studied application. The basic appearance of stick-slip oscillations in Filippov's approach to piecewise-smooth systems is well established, but the role of nonlinear terms at the discontinuity, the introduction of hysteresis, and their perturbation under smoothing and noise, are less well understood.

One enduring challenge in seeking a mathematical understanding of friction between solid bodies is the combined nonlinear and multi-scale nature of the processes involved (see e.g. [38,44,51,53]), and this is typical of interactions not only in mechanics, but in other physical, chemical and biological systems (e.g. [5,18, 22,31,33,40]). One approach is to take both features to their extreme limit by collapsing certain of the nonlinearities and faster timescales into a sharp event: a discontinuity. A parameter in the system is taken to switch abruptly as a quantity v changes sign, say $\mu = \text{sign}(v)$. This carries with it the expectation that the true system to lies 'close to' the switching model, perhaps via a regular perturbation

$$\mu(v) \sim \text{sign}(v) + \mathsf{O}\left(\varepsilon\right) \tag{1}$$

or perhaps a singular perturbation

$$\mu(v) \sim \text{sign}(v) + \mathsf{O}\left(\varepsilon/v\right) \ , \tag{2}$$

each for some small $\varepsilon > 0$ and for all v. The values before and after the switch ($v < 0$ and $v > 0$) are well-known, whereas the complexity of the transition means the precise value at $v \approx 0$ is unknown, and crucially one seeks reasonable arguments to define a value or set of values for $\mu(0)$.

Whether we choose the viewpoint of a regular (1) or singular (2) perturbation implicitly determines the class of discontinuous systems we can study for $\varepsilon = 0$. The former is limited to a direct switch, figure 1(i), and can be studied using the theory of piecewise-smooth (or *Filippov*) dynamical systems [18,25]. The latter, however, is free to explore wider values at the discontinuity because of the singularity in the $\mathsf{O}\left(\frac{\varepsilon}{v}\right)$ term, permitting the generalization shown in figure 1(ii), and also richer dynamics in transitions between $v > 0$ and $v < 0$. To solve a discontinuous system with such a switch requires 'blow up' methods introduced in [34], which we provide a formal derivation for here, giving a subtle but propitious extension of standard theory which can incorporate, for example, hysteretic effects as in figure 1(iii) without having to smooth or otherwise 'regularize' the discontinuity (for references to regularization see see e.g. [49,52], the relation between blow up and regularization is described in [41]). In doing so we show that the distinction between the regular and singular perturbations as a motivation of discontinuous models is essential, because although they differ formally only at $v = 0$, they can give rise to entirely different global dynamics, as we will show.

Various features illustrated in figure 1 — discontinuity in (i), static overshoot in (ii), and hysteresis in (iii) — still form the prevailing model of friction (along
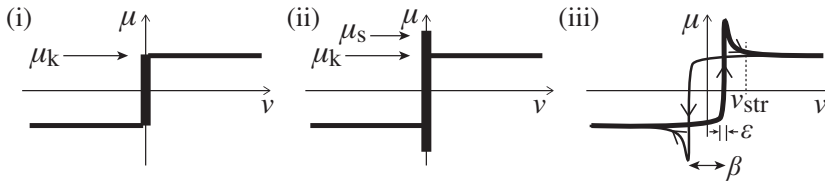
Fig. 1 Switching characteristics for friction: (i) Coulomb model for kinetic friction, (ii) static friction coefficient μ_s exceeds kinetic coefficient μ_k, (iii) smoothed-out law including hysteretic "friction memory" over a scale β, speed dependence up to a Stribeck speed v_{str}, and smoothing over a scale ε. Qualitatively (iii) tends to (ii) as we let $\beta, \varepsilon, v_{\mathrm{str}} \to 0$, and (i) is regained if we also let $\mu_s \to \mu_k$. To understand the difference on the dynamics of a system requires close consideration of how discontinuities (i) or (ii) affect the dynamics of a system.

with an independence of contact area and proportionality to normal load), because refinements seem not to retain the same universal applicability. The classic model of friction attributed to Amontons and Coulomb are of the form in figure 1(i). Complex microscale interactions over the body-to-body interface are modelled by a force that is speed independent, except for a flip of direction as the slip velocity between two surfaces passes through zero. The discontinuity arises from the observation that the kinetic friction force depends on the direction but not the magnitude of the slip velocity v (approximately), so its value jumps, say from $+\mu_k N$ to $-\mu_k N$ under a normal load N, as v passes through zero. The force is assumed to pass only through values on the interval $[-\mu_k N, +\mu_k N]$, the friction cone, when $v = 0$.

An attraction of such a model is that it captures one feature that smoothly differentiable models cannot, namely the irreversibility of stick-slip dynamics. Although the onset of sticking can be predicted uniquely, once sticking occurs it is not possible to infer uniquely when (or even if) slipping occurred in the past. The information required to reverse stick-slip motion is lost to the environment through heat and sound, and it remains a challenge to show how the small, and even atomic, scale, interactions involved in this (e.g. [4,26,38,42,46,55]) reproduce large scale dynamics. A full characterization of these problems is beyond our scope here, though we refer to the literature a little further in section 9. Our purpose is to investigate how much of the bulk behaviour can be qualitatively captured by a discontinuous model, and for completeness, to show that such a model is robust to smoothing of the discontinuity.

Throughout this paper we will assume a known constant normal contact force N, or at least take a constant reference force N (balancing the object's weight, for example), with any complexities in the normal reaction forces on an object taken inside the friction coefficient μ for our purposes.

In neglecting various details of the fine structure physics involved, the model in figure 1(i), which is set-valued at $v = 0$ seems to fail in two respects. Firstly, the friction force takes one *kinetic* value μ_k during slipping contact and another *static* value μ_s when the surfaces stick together, (figure 1(ii)), meaning in practice that the breakaway force required to instigate slipping between two surfaces is greater than that required to maintain slip, an observation made first perhaps by Euler. The coefficients μ_k and μ_s differ for some, though not all, materials and experimental set ups. Secondly, (i) neglects features such as hysteresis (figure 1(iii)). To

compound this mathematically, these problems manifest precisely where the contact force suffers the discontinuity, where the graph of $\mu(v)$ becomes vertical and therefore the value of μ ambiguous. Dealing with that ambiguity one must make certain choices, such as imposing complementarity constraints [11] or sliding rules [25]. We will show that giving formal expression to these ambiguities via nonlinear switching terms leads to rich dynamics encompassing all behaviour in figure 1 in a closed form discontinuous dynamical system.

While any of (i), (ii), or (iii), may be 'better' models given different physical situations, the aim here is a more *general* dynamical approach to the discontinuity, and in this regard to define a model in which (iii) reduces to (ii) in a definite (though singular) limit, preserving the static friction overshoot, which reduces to (i) in another limit, with the simplest mathematical assumptions possible.

The static friction overshoot is to be encoded in 'nonlinear switching' terms suggested by the $\mathsf{O}\left(\varepsilon/v\right)$ term in (2), and we will show its effect on the piecewise-smooth dynamics in the discontinuous limit $\varepsilon = 0$. We do this by first deriving a model of discontinuity from the singular perturbation point-of-view in section 2, then apply it to a simple dry-friction oscillator in subsequent sections, showing how it allows us to introduce static-versus-kinetic friction, hysteresis, compliance and noise, step by step into a discontinuous dynamical system. Conditions for linear and nonlinear sticking are derived in section 5. The dynamics of the system is sketched for the discontinuous model in section 6, requiring some application of perturbation theory whose main technical points we give in section 7; similar methods are employed for genetic networks in [40], where sigmoidal *Hill* functions limit towards jumps similar to that in figure 1(i). Numerical simulations follow in section 8 for the purposes of illustration, comparing the friction characteristic to the features summarized in figure 1, and showing some novel dynamics related to nonlinear terms responsible for static friction. Closing remarks are made in section 9.

This study builds on a growing general understanding of dynamical systems which, like friction, exhibit discontinuities, and will show that some of the complexities of friction are a natural accompaniment to dynamical switching. In doing so we find out what aspects are inherent in a discontinuous model, what dynamics arises only when smoothing out the discontinuity, and what behaviours of a discontinuous model are robust to perturbations like smoothing and noise.

2 From multi-scale oscillation to bulk-scale switching

It is not difficult to see how small-scale complexity can manifest as discontinuity on a large scale, but as we can show with a heuristic but quite general argument, the result is of the singular kind (2) rather than the regular (1).

To obtain a tractable model of the complex contact interactions involved in dry-friction (as we review briefly in section 9), let us say only that they result in a continuum of constitutive forcings, whose distribution over some variable k has an envelope $a(k)$, and an oscillatory part with phase $\theta(k)$. For a specific example we might consider phonons which contribute overall to the friction force with amplitudes $a(k)$ and relative phases $\theta(k)$. We take a and θ to be real continuous and even functions of k, such that positive and negative k represent forcings in opposite directions; these assumptions are not too important and partly for simplicity. More

crucially we assume that these forces are excited by motion of the bulk system, represented by a quantity v, resulting in a cut-off at some $k_* = v/\varepsilon$ for $\varepsilon > 0$. In this way we write the interaction force integrated over all k as $N\mu(v)$, where N is a normalization constant and

$$\mu(v) = \frac{1}{\sqrt{2\pi}} \int_0^{v/\varepsilon} dk\, a(k) \cos\theta(k) \ , \tag{3}$$

(the factor $\frac{1}{\sqrt{2\pi}}$ is inserted for convenience). Asymptotic expansions of such integrals often produce Stokes' discontinuities (see Appendix A), found via stationary phase methods to be of a typical form

$$\mu(v) \sim r\,\mathrm{sign}(v) + q(v/\varepsilon) \sum_{n=0}^{\infty} \frac{c_n}{(v/\varepsilon)^{2n}} \tag{4}$$

in terms of a smooth function q, coefficients c_n, and a constant $r = \mathrm{Re}\left[\frac{a(k_s)e^{i\theta(k_s)}}{\sqrt{-\psi''(k_s)}}\right]$ where $\psi = i\theta + \log a$ and $\psi'(k_s) = 0$. This series is of the form (2) up to the constant r, which can be absorbed into N. For more general discussion of such classes of integrals and the Stokes' phenomena they produce see also [7,20,50].

The graph shown in figure 2(i) is typical of (3), and tends towards a curve like figure 2(ii) in the limit $\varepsilon \to 0$, which has peak values $\mu = \pm\mu_s$ which are ε-independent and therefore remain clearly defined in the limit $\varepsilon \to 0$. (In the example of Appendix A the peak has height $\mu_s \sim 1 + \sqrt{\frac{2}{\pi}\frac{4\rho^3}{\pi^2}}\,e^{-\pi^2/8\rho^2}$ and lies at $v \sim \pm\pi\varepsilon/2\rho$).
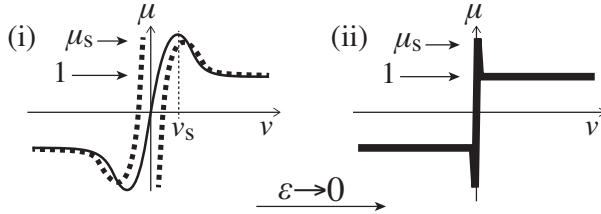

Fig. 2 The contact coefficient μ integrated over a gaussian force distribution $a(k)$: (i) shows the exact integral (3) (full curve) for $a(k) = e^{-k^2/2}$ and $\theta(k) = 3k/2$, along with the asymptotic approximation (dotted curve) up to the first term of the series in Appendix A (37); in (ii) this tends towards a step function with ε-independent spikes at $v = 0$ in the limit of small ε.

Neglecting r, we can express (4) as

$$\mu(v) \sim \Lambda_\varepsilon(v) + \rho L_\varepsilon(v)\Gamma_\varepsilon(v) \xrightarrow{\varepsilon \to 0} \Lambda(v) + \rho L(v)\Gamma(v) \tag{5}$$

(as described further in Appendix A). The function Λ_ε is differentiable and monotonic and satisfies

$$\Lambda_\varepsilon(v) \in \left\{ \begin{array}{ll} \mathrm{sign}(v) + \mathsf{O}\,(\varepsilon) & \text{if } |v| > \varepsilon \\ [-1,+1] & \text{if } |v| \leq \varepsilon \end{array} \right\} \xrightarrow{\varepsilon \to 0} \Lambda(v) \in \left\{ \begin{array}{ll} \mathrm{sign}(v) & \text{if } v \neq 0 \\ [-1,+1] & \text{if } v = 0 \end{array} \right\} , \tag{6}$$

while Γ_ε is differentiable and satisfies

$$\Gamma_\varepsilon(v) \in \left\{ \begin{matrix} \mathsf{O}\left(\frac{\varepsilon}{v}\right) & \text{if } |v| > \varepsilon \\ (0,1] & \text{if } |v| \leq \varepsilon \end{matrix} \right\} \quad \xrightarrow{\varepsilon \to 0} \quad \Gamma(v) \in \left\{ \begin{matrix} 0 & \text{if } v \neq 0 \\ (0,1] & \text{if } v = 0 \end{matrix} \right\} . \tag{7}$$

For example we may fix

$$\Gamma_\varepsilon(v) = 1 - \Lambda_\varepsilon^2(v) . \tag{8}$$

The constant ρ is related (in a way that must be determined later) to the peak height of the integral and therefore to μ_s; we relate ρ and μ_s in a particular example later. This leaves the function L_ε. For brevity in this paper we consider only the case $L_\varepsilon = \Lambda_\varepsilon$ (and hence $L = \Lambda$).

In (5), the function Λ directly replaces the sign term from (4), and when defining it in (6) we take care to specify its range at $v = 0$, where it is set-valued. The second term of (5) embodies the tail of the asymptotic approximation (4), with the factor Γ contributing only where Λ switches sign, i.e. in the static mode $v = 0$; the static contribution has a strength ρ.

While the functions $\Lambda_\varepsilon(v)$ and $\Gamma_\varepsilon(v)$ are continuous and single-valued, their limits Λ and Γ are set-valued at $v = 0$, and it is useful to identify their values in the sticking mode with new variables λ and γ, given by

$$\lambda \equiv \Lambda(0) \in [-1, +1] \qquad \text{and} \qquad \gamma \equiv \Gamma(0) \in (0, 1] . \tag{9}$$

(These can be called 'selections' of the set-valued terms. If we neglect γ then this in effect consistent with standard Filippov theory [25, 18, 39]). Differentiating (6) and comparing to (7) we can write asymptotically that $\varepsilon \frac{d}{dv}\Lambda_\varepsilon(v) = \Gamma_\varepsilon^p(v) + \mathsf{O}\left(\varepsilon/v\right)$ where p is some positive exponent, and use this to relate λ and γ formally via

$$\frac{d\Lambda}{dv} = \lim_{\varepsilon \to 0} \frac{\Gamma_\varepsilon^p(v)}{\varepsilon} \quad \Rightarrow \quad \frac{d\Lambda}{dv/\varepsilon} = \Gamma^p(v) \quad \Rightarrow \quad \frac{d\lambda}{dv/\varepsilon} = \gamma^p(\lambda) . \tag{10}$$

This relation will be of use later. In Appendix A and in simulations in section 8 we choose $\Lambda_\varepsilon(v) = \frac{v/\varepsilon}{\sqrt{1+(v/\varepsilon)^2}}$, which gives (10) with $p = 3/2$.

Functions of the form (6) are rather common in physical and biological models as sigmoid functions describing switches or fast transitions, and it is common to approximate them with a sign function with little regard for what forms of behaviour are possible at $v = 0$. The purpose of this paper is to show that the piecewise-smooth systems implied by the argument above — specifically containing nonlinear dependence on Λ via Γ — lie outside the standard theory of piecewise-smooth systems [25], but can be handled with a straightforward extension [34] which makes that theory more widely applicable, and we present such an application in the form of static friction.

3 A near steady-state model

The basic problem of interest is that of an object of mass m, resting on a surface which exerts on it a normal reaction force N, and subjected to forces $b(x, \dot{x}, t)$ that drag the object along the surface. This satisfies the one degree of freedom system

$$m\ddot{x} = b(x, \dot{x}, t) - \mu(v)N , \tag{11}$$

where x is the object displacement, $\dot{x}$ its velocity, and v is the velocity of slip relative to the surface. The friction coefficient μ is an odd function of the slipping speed v.

We have then to form a model for the friction coefficient $\mu(v)$. The asymptotic models in section 1 have a leading order term $\mu(v) = \text{sign}(v)$, which is clearly consistent with Coulomb's laws of kinetic friction (figure 1(i)). Let us then assume, as suggested in the introduction, that this is only the leading order term of some approximation of the form (2) for small ε. We shall use the form of μ derived in section 1, namely (5) using (6)-(7). The ε-dependent expressions are not vital for the subsequent analysis in this paper, but we carry them along throughout to show where the discontinuous ($\varepsilon = 0$) expressions come from, and in section 7 give some basic theorems on the persistence of the discontinuous system for $\varepsilon > 0$.

The description so far assumes a stationary model for the friction coefficient, requiring the contact surface to be in some overall steady state during slip. If small motions produce variations away from (5), we may consider Γ to be only the equilibrium position of a surface variable z, and thus write instead of (5) as a first approximation,

$$\mu(v) = \Lambda(v) + \rho\Lambda(v)z \tag{12}$$

where z relaxes to Γ on a fast timescale $t \approx \beta$ for small $\beta > 0$, given by

$$\beta\dot{z} = \Gamma(v) - z \tag{13}$$

linearized around the steady state $z = \Gamma(v)$.

Within the dynamical system (11), equations (12)-(13) now form the friction model, endowed with discontinuity by Λ, nonlinearity by Γ, and relaxation by z. We recall that the kinetic coefficient of friction for large $|v|$ has been scaled to unity, and static friction enters via the terms with coefficient ρ. It will turn out that β introduces hysteresis on the timescale $t \approx \beta$. The parameter ε plays only a practical role in the definition of the discontinuous functions (6)-(7), but later will become associated with compliance.

4 A friction oscillator

Below we show the different aspects of the model (12)-(13) in the context of a single degree of freedom oscillator used in experimental studies of friction (e.g. in [55], or for alternatives see [6,30]). A schematic model is shown in figure 3. The set up consists of an object of mass m, supported via two springs with total spring coefficient k, mounted on a shaking base plate with a controllable displacement $q(t)$. Friction between the object and the plate is introduced via a vertical sliding contact, typically attached to a force transducer. Contact between the base and the mass also introduces a linear damping coefficient c, so that the non-frictional forces on the mass add up to

$$b(x, \dot{x}, t) = -(x - q)k - (\dot{x} - \dot{q})c . \tag{14}$$

The relative displacement between the object and the plate is then $y = x - q$, the relative velocity $v = \dot{y} = \dot{x} - \dot{q}$, for which we obtain from (11) a differential inclusion

$$\begin{aligned} \dot{y} &= v , \\ \dot{v} &= \ddot{q} - ky - cv - N\mu(v) , \end{aligned} \tag{15}$$
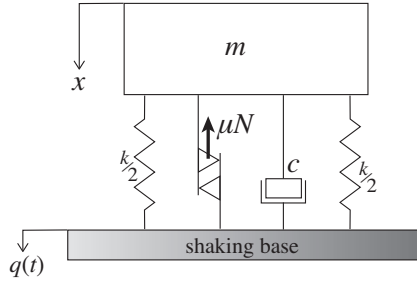
Fig. 3 Schematic of the bouncer, a base plate shaken vertically with displacement $q(t)$, transmitted to an object mass m via total spring constant k, dashpot coefficient c, and friction slider with normal load N and dry-friction coefficient μ.

along with (12)-(13) as a friction model. Here we have re-scaled so that $m = 1$. For simulations we will also let $N = 1$, and apply a driving oscillation $\ddot{q}(t) = -\sigma \sin \omega t$ through the base with amplitude σ and frequency ω.

5 Linear vs. Nonlinear sticking

A basic task in such a system is to determine when sticking will occur. This happens at displacements $y(t)$ for which $v = \dot{v} = 0$ is a solution of the system (15) for $\Lambda(0) \in [-1, +1]$, in which case the system evolves along the discontinuity surface $v = 0$, and using (9) we replace the function values $\Lambda(0), \Gamma(0)$, with variables $\lambda, \gamma(\lambda)$. We shall see how to derive the dynamics of these variables in the next section, here we ask merely whether sticking solutions exist for some $\lambda \in [-1, 1]$ at a given y and t.

For $\rho = 0$ the friction coefficient μ depends linearly on λ, in fact $\mu = \lambda$ by (12), so that the sticking conditions $v = \dot{v} = 0$ in (15) for $\lambda \in [-1, +1]$ imply $|ky - \ddot{q}| < N$. We will refer to the dynamics in this region as *linear sticking*. The boundaries correspond to the maximum and minimum of the graph $y = \frac{1}{k}(\ddot{q} - N\lambda)$ which lie at $\lambda = \pm 1$. Linear sticking is equivalent to applying Filippov's convex combination to find regions of so-called 'sliding' along the threshold $v = 0$ [25]. The boundaries of the linear sticking region are the set of tangency points of the right and left subsystems to the discontinuity surface, i.e. where $\lim_{\delta \to 0} \dot{v}|_{v=\pm\delta} = 0$ for some $\delta > 0$, which yields boundary curves $ky = \ddot{q} \mp N$ on $v = 0$.

For $\rho \neq 0$ the sticking conditions $v = \dot{v} = 0$ with $\lambda \in [-1, +1]$ instead give $|ky - \ddot{q}| < (1 + \rho z)N$. Thus the variation of z implies that sticking may now occur for a larger range of y and t, which we refer to as *nonlinear sticking*. The boundaries correspond to maximum and minimum of the graph $y = \frac{1}{k}(\ddot{q} - N\lambda(1 + \rho z))$ as it varies over $\lambda \in [-1, +1]$, which now might not occur simply at $\lambda = \pm 1$, but may lie instead at turning points of the graph if they exist inside $\lambda \in [-1, +1]$.

If we assume z has reached its steady state value Γ, which on $v = 0$ becomes γ by (9), then the turning points of $y = \frac{1}{k}(\ddot{q} - N\lambda(1 + \rho\gamma(\lambda)))$ lie at any $\lambda = \pm\lambda_s \in [-1, +1]$ such that

$$\frac{d\mu(\lambda_s)}{d\lambda} \equiv 1 + \rho\gamma(\lambda_s) + \rho\lambda_s \frac{\partial\gamma(\lambda_s)}{\partial\lambda} = 0 \, . \tag{16}$$

For a basic friction model it will be sufficient to assume (as we do hereon) that (16) has at most one symmetric pair of solutions $\pm\lambda_s$; see figure 4. Substituting this into $\mu = \lambda(1 + \rho\gamma)$ gives peak values of the friction coefficient as $\mu = \pm\mu_s$ where

$$\mu_s := \begin{cases} -\rho\frac{d\gamma(\lambda_s)}{dv}\lambda_s^2 & \text{if } |\lambda_s| < 1 \,, \\ 1 & \text{if } |\lambda_s| \geq 1 \,, \end{cases} \tag{17}$$

and corresponding y-bounds on the sticking region as $\frac{1}{k}(\ddot{q} - N\mu_s) < y < \frac{1}{k}(\ddot{q} + N\mu_s)$. This determines the maximum force of static friction $\mu_s N$, and thus sets the maximum size of the nonlinear sticking region.
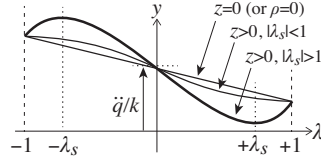

Fig. 4 The graph $y = (\ddot{q} - N\mu(\lambda))/k$ where $\mu(\lambda) = \lambda(1 + \rho\gamma(\lambda))$, over $\{y, \lambda\} \in \mathbb{R} \times [-1, 1]$. If $|\lambda_s| < 1$ the graph has peaks $y = (\ddot{q} - N\mu_s)/k$ at $\lambda = \pm\lambda_s$, otherwise its peak values lie at $\lambda = \pm 1$.

Putting the two cases together, we identify regions of sticking depending on whether we exclude nonlinear terms ($\rho = 0$) or include them ($\rho \neq 0$), defining:

$$\text{linear sticking where} \quad v = 0 \quad \& \quad |ky - \ddot{q}| \leq N \qquad \text{for } \rho = 0 \,, \tag{18}$$
$$\text{nonlinear sticking where} \quad v = 0 \quad \& \quad |ky - \ddot{q}| \leq N\mu_s \quad \text{for } \rho \neq 0 \,. \tag{19}$$

In physical terms, ignoring the driving term $\ddot{q}$, these mean that the force ky the spring must exert to overcome friction and cause breakaway from sticking is $\pm N$ or $\pm\mu_s N$ in the linear or nonlinear models respectively. To produce peaks in μ, the even function γ must be at least of quadratic order in λ. If we assume for example that $\gamma(\lambda)$ is a quadratic polynomial, the requirement $\gamma(\pm 1)$ fixes $\gamma(\lambda) = 1 - \lambda^2$ (consistent with (8)). Then $\lambda_s = \sqrt{(1 + \rho)/3\rho}$ giving $\mu_s = 2\rho((1 + \rho)/3\rho)^{3/2}$ for $\rho > 1/2$ and $\mu_s = 1$ for $\rho \leq 1/2$.

In standard theory with $\rho = 0$, solving the sticking conditions $v = \dot{v} = 0$ is sufficient to find the value of λ that corresponds to sticking dynamics. If we take $\rho \neq 0$ and include nonlinear dependence on λ, however, the sticking conditions $v = \dot{v} = 0$ may lead to multiple sticking solutions. Nonlinear sticking therefore requires dynamical theory introduced in [34], which we present in the next section. This will include finding rich dynamics appears in the regularization of the discontinuity. For example, the boundaries of the nonlinear sticking region are associated with loss of hyperbolicity in the dynamics of $\{y, z, \lambda\}$ treated as independent variables.

6 Piecewise-smooth dynamics

In slipping motion we have $v \neq 0$ so the system relaxes quickly (in time $t = \mathsf{O}(\beta)$) to a state $\mu(v) = \Lambda(v) = \text{sign}(v)$, then the dynamics of (15) is rather simple to sketch as in figure 5 (vertical planes). Viewed in the y-v plane (imagining z and

t fixed), the flow curves towards $v = 0$ from both slipping regions. Similar phase portraits appear in e.g. [30], and motion outside of sticking is relatively simple.

In between slipping directions we must resolve the dynamics in the discontinuity surface $v = 0$. For this we require the rate of change of the λ variable, and as stated in [34], it rather easily given relative to some dummy timescale as $\lambda' = \dot{\mathbf{x}} \cdot \nabla v$ where $\mathbf{x} = (t, y, v)$ and ∇ is its associated gradient operator. This result appeared in [34] and we give a more detailed justification here, with a formal derivation (below) using the dummy infinitesimal ε.

The time derivative of λ is given, using (10), by

$$\dot{\lambda} = \dot{v} \frac{d\lambda}{dv} = \dot{v} \gamma^p / \varepsilon \; . \tag{20}$$

As the dot denotes differentiation with respect to a time t, equation (20) says that λ evolves on a timescale $\tau = t\gamma/\varepsilon$. Letting $\gamma \in (0, 1]$ remain fixed as $\varepsilon \to 0$, the timescale τ is fast compared to t. Substituting $v = 0$ into the dynamical system (15), recalling $\gamma(\lambda) \neq 0$ for $v = 0$ and denoting the derivative with respect to $\tau = t\gamma/\varepsilon$ with a prime, we have a 'fast' system

$$\left. \begin{array}{l} t' = \frac{\varepsilon}{\gamma(\lambda)} \\ \lambda' = \ddot{q} - ky - N\mu(v) \\ \beta z' = \gamma(\lambda) - z \end{array} \right\} \xrightarrow{\varepsilon \to 0} \left\{ \begin{array}{l} t' = 0 \\ \lambda' = \ddot{q} - ky - N\lambda\,(1 + \rho z) \\ \beta z' = \gamma(\lambda) - z \end{array} \right. , \tag{21}$$

substituting in $\mu = \lambda\,(1 + \rho z)$ by (12) on the righthand side. This fast dynamics is sketched (double arrows) in figure 5 in the steady state $z = \gamma(\lambda)$, in the $v = 0$ plane which represents $\{t, \lambda, z\}$ space. The discontinuous (i.e. $\varepsilon = 0$) system consists of a $\{t, y, z\}$-parameterized one-dimensional system with a three-dimensional surface of equilibria

$$\mathcal{B}(z) = \left\{ (t, y, z, \lambda) \in \mathbb{R}^3 \times (-1, +1) : \; \ddot{q} - ky - N\lambda\,(1 + \rho z) = 0 \right\} \; . \tag{22}$$

The manifold $\mathcal{B}$ is coordinatized by $\{t, y, \lambda\}$, while z determines its shape. In $\{y, \lambda\}$-space, $\mathcal{B}(0)$ is a straight line with y-intercept $\ddot{q}/k$, and

$$\mathcal{B}_\gamma \equiv \mathcal{B}(\gamma(\lambda)) \tag{23}$$

is a curve with turning points at $\lambda = \pm\lambda_s$ if $|\lambda_s| < 1$ as defined by (16); these are just the curves shown in figure 4.

If a trajectory spends a sufficient time $t = \mathsf{O}\,(\beta)$ inside $v = 0$, the variable z will relax to $\gamma(\lambda)$ and hence $\mathcal{B}(z)$ will relax to $\mathcal{B}_\gamma$. A brief consideration of the sign of $\frac{\partial \lambda'}{\partial \lambda} = -N\left(1 + \rho\gamma(\lambda) + \rho\lambda\frac{d\gamma(\lambda)}{d\lambda}\right)$ shows that $\mathcal{B}_\gamma$ always has an attracting branch (where $\frac{\partial \lambda'}{\partial \lambda} < 0$) over $|\lambda| < \min[\lambda_s, 1]$, using λ_s defined in (16), onto which the system collapses on the timescale τ. If $|\lambda_s| < 1$ then $\mathcal{B}(z)$ also has two repelling branches over $\lambda_s < |\lambda| < 1$, with the attracting and repelling branches separated by sets of turning points at $\lambda = \pm\lambda_s$, as depicted in figure 5.

The equation $t' = 0$ in (21) means that this fast τ-timescale dynamics is instantaneous on the 'slow' timescale t, consisting of collapse to $\mathcal{B}(z)$ for y values inside the sticking region (19), instigating sticking motion, while for y values outside this λ will switching between $\lambda = \pm 1$ which signifies the transition between left and right slip.
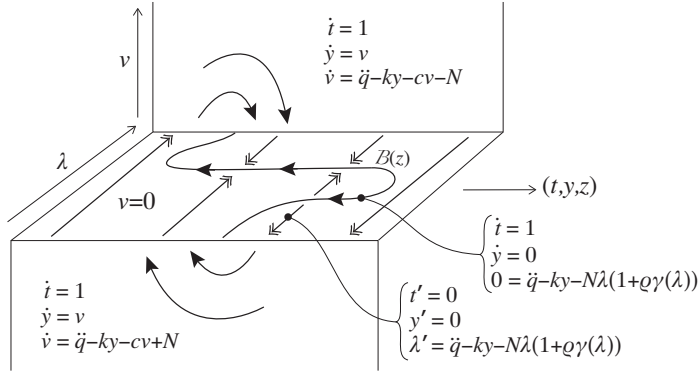
Fig. 5 Discontinuous model showing: slipping in the vertical panels representing dynamics in $\{y, v, t\}$ variables (given by (15) with (6)); fast transition given by (21) in the surface $v = 0$; sticking in the surface $\mathcal{B}(z)$ with dynamics in λ given by (24). The equations shown are for the steady state $z = \gamma(\lambda)$. For an example of γ consider $\gamma(\lambda) = 1 - \lambda^2$.

Dynamics inside $\mathcal{B}(z)$ takes place on the timescale t, given directly by setting $v = 0$ in (15) and using (20) to find $\dot{\lambda}$, as

$$
\left.
\begin{aligned}
\dot{t} &= 1 \\
\tfrac{\varepsilon}{\gamma(\lambda)}\dot{\lambda} &= \dot{v} = \ddot{q} - ky - N\mu(v) \\
\beta z' &= \gamma(\lambda) - z
\end{aligned}
\right\}
\xrightarrow{\varepsilon \to 0}
\left\{
\begin{aligned}
\dot{t} &= 1 \\
0 &= \ddot{q} - ky - N\lambda\,(1 + \rho z) \quad . \\
\beta z' &= \gamma(\lambda) - z
\end{aligned}
\right.
\tag{24}
$$

The second line simply constrains the dynamics to $\mathcal{B}(z)$ by (22), and implies $\dot{v} = 0$, hence motion in $\mathcal{B}(z)$ represents sticking. The arrows inside $\mathcal{B}(z)$ in figure 5 indicate that sticking trajectories tend to move towards or away from the extrema of $\mathcal{B}(z)$, simply because the position of $\mathcal{B}(z)$ itself moves if $\ddot{q}$ (and thereby (22)) is t-dependent.

Trajectories of the full system transition between the subsystems (15), (21) and (24). Left-slip or right-slip obey (15) with $v \neq 0$. Switches between the two are made via the fast system (21), as shown by trajectory (i) in figure 6. For $\{y, t\}$ values that fall within (19), the fast system collapses to $\mathcal{B}(z)$, and sticking dynamics ensues given by (24). This sticking dynamics continues while (19) is still satisfied, otherwise the system transitions via the fast system back into slipping, as shown by trajectory (ii) in figure 6.
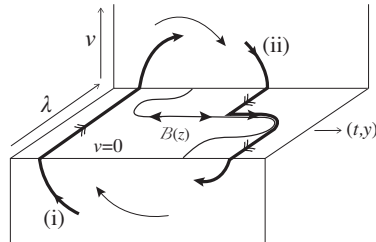

Fig. 6 Discontinuous model showing transitions. Trajectory (i) transitions between slipping motion (vertical panels) via the fast system (double arrows). Trajectory (ii) transitions between slipping motion but undergoes an interval of sticking on the manifold $\mathcal{B}(z)$.

To plot the friction characteristic $\mu(v)N$ for this system for comparison with figure 1, consider a solution of the oscillator system which oscillates through both slipping regions $v > 0$ and $v < 0$, with sticking in between. This yields graphs of the form of figure 7(i) for $\lambda_s < 1$, with peaks that are clearly consistent with the existence of static friction, whose heights are given by (17) and prescribe the maximum coefficient of static friction.

The arrows in figure 7(i) come from considering how the dynamics will explore the graph subject to the relaxation (13). We obtain them by heuristic argument, but will verify them with simulations in the next section. During slipping the system approaches $z \approx \Gamma = 0$, so the friction coefficient (12) has no peaks and does not exhibit static friction. Entering into stick or changing slipping direction, therefore, the friction coefficient transitions directly between ± 1. During an interval of sustained sticking, however, z will grow sharply by (13) to a value $z \in (0,1]$, and if $\lambda_s < 1$ then the coefficient (12) approaches $\mu \to \lambda\left(1 + \rho\gamma(\lambda)\right)$ as $z \to \gamma \equiv \Gamma(0)$, which has peaks at $\lambda = \pm\lambda_s$. For the system then to exit back into slip from $v = 0$ to $v \neq 0$ it must pass through these peaks in the friction coefficient at $|\mu| = \mu_s = -\lambda_s^2 \frac{d\gamma(\lambda_s)}{dv} > 1$, forming the spikes in figure 7(i). The static friction response is therefore hysteretic.

The model sketched in figure 7(i) reproduces the phenomena of static friction and hysteresis presented in figure 1, but it lacks two features shown in figure 1(iv), namely a separation between the two vertical branches of the friction graph, and smoothing. Both can now be attributed to compliance effects outside the discontinuous model of the contact force. The model so far assumes the object mass to be a point particle, but let us suppose that the object is an extended body, which in resisting the contact force suffers a small shear proportional to the spring extension y, so that instead of v we plot a measured velocity of $\bar{v} = v - \varepsilon y$ for small $\varepsilon > 0$. The effect on the characteristic is shown in figure 7(ii). The different branches of the hysteresis loop are revealed, capturing all of the behaviour suggested in figure 1(iv) except for smoothing. Smoothing is now achieved by replacing Λ and Γ with smooth functions Λ_ε and Γ_ε (and let us assume the two instances of ε in this paragraph are the same); this will follow below.
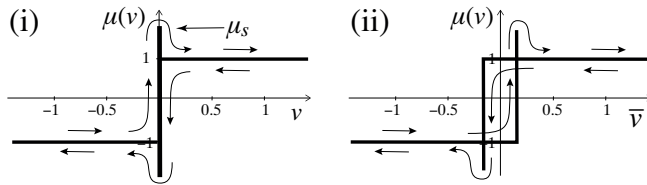

Fig. 7 Friction characteristic for the bouncer, discontinuous model plotted against the relative speed v in (i), and against the offset speed $\bar{v} = v - \varepsilon y$ representing compliance in (ii). Places where the graph is horizontal correspond to slip, and where it is vertical corresponds to stick.

These sketches of the characteristics can be confirmed by numerical simulation, which we perform in section 8. One may simulate the discontinuous model directly, using event detection methods to switch between the four subsystems summarized in figure 5. There are packages already programmed for solving ordinary differential equations with switching (e.g. [45,19]), but current event detection routines

typically assume Filippov-type solutions and would thus neglect the crucial non-linear terms $\gamma(\lambda)$.

A simpler recourse than event detection sufficient for our purposes here, and a usually reliable one (if stiff numerically), is to simulate using a standard numerical ordinary differential equation solver, which requires replacing the discontinuous function (6) with a smoothed-out sigmoidal curve with a slope sufficiently steep to approximate the sign function (see e.g. [30]). The way to do this is already suggested by the definitions (6)-(7), and has the added effect of emulating, though rather crudely, any smoothing of the switching process arises through compliance of the object and surface, and provides the final visual ingredient to reproduce all aspects of figure 1. As a numerical tool we do not advocate the use of smoothing, but it fits the analytical context here, particularly our interest in the asymptotics and geometry behind frictional switching. For studies focussed on the numerical results themselves, event detection or event capturing may be more appropriate, see e.g. [12,13], but will require some consideration as to how to handle nonlinear switching.

Before proceeding to a numerical simulation we verify that the dynamics as sketched above is robust, by means of a few technical details regarding the perturbation to $\beta > 0$ and $\varepsilon > 0$.

7 Perturbation to $\beta > 0$ and $\varepsilon > 0$

Gathering together equations (15) and (12)-(13), the complete equations of the discontinuous system are

$$\left.\begin{array}{l} \dot{t} = 1 \\ \dot{y} = v \\ \dot{v} = \ddot{q} - ky - cv - N\Lambda(v)\left(1 + \rho z\right) \\ \beta \dot{z} = \Gamma(v) - z \end{array}\right\} \qquad (25)$$

for small $\beta > 0$, in terms of variables $\{y, v, z\}$ and the functions $\Lambda(v)$, $\Gamma(v)$, from (6)-(7). On $v = 0$ the values $\Lambda(0)$ and $\Gamma(0)$ shall be replaced by dummy variables λ and $\gamma(\lambda)$ according to (9). For $N\mu_s \geq \max|\ddot{q}(t)|$ the system (25) exhibits sticking periodic orbits, and otherwise stick-slip or pure slipping periodic orbits are expected; these are discussed briefly in Appendix B.

To understand the system above in practice it is desirable to know how robust it is to perturbations. For example, what happens if we smooth out or stochastically 'blur out' the discontinuity? The effects of noise will be considered in section 8. The remainder of this section considers the effects of smoothing, adapting standard notions of fast and slow dynamics from geometric singular perturbation theory [24, 36] to show essentially that, if Λ and Γ are replaced by Λ_ε and Γ_ε according to (6) and (7), we obtain dynamics that is ε-close to the discontinuous dynamics of (25) as described in the previous section.

The third line of (25) introduces a relaxation towards $z = \Gamma(v)$ on the fast timescale t/β. The state $z = \Gamma(v)$ is invariant for motion confined to either $v < 0$, $v > 0$, or $v = 0$, but is not invariant to motion that transitions between them, because the attractor $z = \Gamma(v)$ is discontinuous; this is the feature that permits hysteresis. One way to see this is to let $w = \Gamma(v) - z$, then $\beta \dot{w} = \beta \dot{v} \Gamma'(v) - w$, which has a well-defined attractor at $w = \beta \dot{v} \Gamma'(v)$. For $\beta \to 0$ this attractor

becomes $w = 0$, except as v approaches zero, in which case $\Gamma' \to \infty$ and $w = 0$ is invariant only if $\beta\Gamma'$ is finite. In (26) below and the subsequent propositions we will make sense of this by smoothing the discontinuity.

The following propositions concern a class of smooth systems which tend to (25) in the limit $\varepsilon \to 0$, namely

$$
\left.
\begin{aligned}
\dot{t} &= 1 \\
\dot{y} &= v \\
\dot{v} &= \ddot{q} - ky - cv - N\Lambda_\varepsilon(v)\,(1 + \rho z) \\
\beta\dot{z} &= \Gamma_\varepsilon(v) - z
\end{aligned}
\right\}
\tag{26}
$$

in terms of functions $\Lambda_\varepsilon(v)$ and $\Gamma_\varepsilon(v)$ which satisfy (6)-(7). To study this will require a number of re-scalings of the 'slow' time variable t to fast times $\tau = t\Gamma_\varepsilon/\varepsilon$, $\tau_\varepsilon = t/\varepsilon$, and $\tau_\beta = t/\beta$, and we shall denote the derivative of a variable x with respect to these fast times by x', x'^ε, and x'^β, respectively.

Let us first consider the relaxation that takes place on the timescale of order β. For $|v| > \varepsilon$ the slow subsystem (26) satisfies

$$
(26) \quad \xrightarrow{\varepsilon \to 0} \quad
\begin{cases}
\dot{t} = 1\,, \\
\dot{y} = v\,, \\
\dot{v} = \ddot{q} - ky - cv - N\operatorname{sign}(v)\,(1 + \rho z)\,, \\
\beta\dot{z} = -z
\end{cases}
\tag{27}
$$

using the limits of Λ_ε and Γ_ε from (6)-(7). Moreover,

$$
(27) \quad \xrightarrow{\beta \to 0} \quad
\begin{cases}
\dot{t} = 1 \\
\dot{y} = v \\
\dot{v} = \ddot{q} - ky - cv - N\operatorname{sign}(v)\,(1 + \rho z) \\
0 = -z
\end{cases}
\tag{28}
$$

prescribes slow dynamics in the surface $z = 0$. The fast dynamics outside $z = 0$ is found by rescaling (26) to the time $\tau_\beta = t/\beta$, denoting the time derivative of any variable x by x'^β, giving

$$
\left.
\begin{aligned}
t'^\beta &= \beta \\
y'^\beta &= \beta v \\
v'^\beta &= \beta\left[\ddot{q} - ky - cv - N\Lambda_\varepsilon(v)\,(1 + \rho z)\right] \\
z'^\beta &= \Gamma_\varepsilon(v) - z
\end{aligned}
\right\}
\xrightarrow{\beta \to 0}
\begin{cases}
t'^\beta = 0 \\
y'^\beta = 0 \\
v'^\beta = 0 \\
z'^\beta = -z
\end{cases}
.
\tag{29}
$$

From the fast β timescale system and its singular limit in (29) we have:

Proposition 1 *Relaxation dynamics in slipping: For $|v| \gg \varepsilon$ the system (26) possesses invariant manifolds $\mathcal{C}_{slip}^{(\beta,\varepsilon)}$ that lie within $\mathsf{O}\,(\beta,\varepsilon)$ of and diffeomorphic to the three-dimensional surface $\mathcal{C}_{slip}^0 = \left\{(t,y,v,z) \in \mathbb{R}^4 : z = 0\right\}$, on which the dynamics is topologically equivalent to the limiting slow subsystem (28).*

Proof The manifold $\mathcal{C}_{slip}^0 = \left\{(t,y,v,z) \in \mathbb{R}^4 : z = 0\right\}$ is the set of normally hyperbolic equilibria of the one-dimensional system (29) with $\beta = \varepsilon = 0$, so by Fenichel's theorem [24,36] the system (27) for $\beta > 0$ possesses locally invariant manifolds $\mathcal{C}_{slip}^{(\beta)}$ that lie $\mathsf{O}\,(\beta)$ close to and diffeomorphic to $\mathcal{C}_{slip}^0$, on which the dynamics is topologically equivalent to the $\beta \to 0$ limit of (28). For $\varepsilon > 0$ and

$|v| > \varepsilon$ the system (26) is an $\mathsf{O}\left(\varepsilon\right)$ regular perturbation of (28), which therefore possesses invariant manifolds $\mathcal{C}_{slip}^{(\beta,\varepsilon)}$ which are an $\mathsf{O}\left(\varepsilon\right)$ perturbation of $\mathcal{C}_{slip}^{(\beta)}$ and therefore lie $\mathsf{O}\left(\beta,\varepsilon\right)$ close to and diffeomorphic to $\mathcal{C}_{slip}^{0}$, exhibiting dynamics which is an $\mathsf{O}\left(\beta,\varepsilon\right)$ perturbation of the slow subsystem (28).

The dynamics in the region $|v| < \varepsilon$ is somewhat richer. It depends acutely on the balance of the small quantities β and ε, and for brevity here we assume $\varepsilon \ll \beta$, since, though β is a small parameter in the model above, ε is a dummy parameter assumed to be arbitrarily small.

First let us consider the relaxation dynamics on $|v| < \varepsilon$. Let $u = v/\varepsilon$, then by (6)-(7) we have $\Lambda_\varepsilon(v) = \Lambda_1(u)$ and $\Gamma_\varepsilon(v) = \gamma_1(u)$, which are functions of u independent of ε. Since $\Lambda_1(u)$ is then a differentiable and monotonic function of u, by the implicit function theorem $\Lambda_1(u)$ has an inverse $u = u(L)$. Therefore let us replace $\Lambda_1(u)$ and $\Gamma_1(u)$ with a dependent variable λ and a function $\gamma(\lambda)$ respectively. The slow dynamics (on the timescale t) is given by (26), which becomes

$$\left. \begin{aligned} \dot{t} &= 1 \\ \dot{y} &= \varepsilon u \\ \varepsilon \dot{u} &= \ddot{q} - ky - c\varepsilon u - N\lambda\left(1 + \rho z\right) \\ \beta \dot{z} &= \gamma_1(\lambda) - z \end{aligned} \right\} . \tag{30}$$

Letting $\varepsilon \to 0$ we obtain sticking dynamics, that is, on the limiting surface $v = \varepsilon u \xrightarrow{\varepsilon \to 0} 0$ we have slow dynamics

$$(30) \qquad \xrightarrow{\varepsilon \to 0} \qquad \left\{ \begin{aligned} \dot{t} &= 1 \\ \dot{y} &= 0 \\ 0 &= \ddot{q} - ky - N\lambda\left(1 + \rho z\right) \\ \beta \dot{z} &= \gamma(\lambda) - z \end{aligned} \right. , \tag{31}$$

the constraint on the third line fixing this dynamics to the surface $\mathcal{B}(z)$ defined in (22). Letting also $\beta \to 0$ we have

$$(31) \qquad \xrightarrow{\beta \to 0} \qquad \left\{ \begin{aligned} \dot{t} &= 1 \\ \dot{y} &= 0 \\ 0 &= \ddot{q} - ky - N\lambda\left(1 + \rho\gamma(\lambda)\right) \\ 0 &= \gamma(\lambda) - z \end{aligned} \right. , \tag{32}$$

which describes slow dynamics after trajectories in the surface $\mathcal{B}(z)$ relax to the surface $\mathcal{B}_\gamma$ defined in (23). Associated with this is a dynamical system on the fast timescale $\tau_\beta = t/\beta$, the derivative with respect to which we denote x'^β for any variable x, giving

$$\left. \begin{aligned} t'^\beta &= \beta \\ y'^\beta &= \varepsilon\beta u \\ \varepsilon u'^\beta &= \left[\ddot{q} - ky - c\varepsilon u - N\lambda\left(1 + \rho z\right)\right]\beta \\ z'^\beta &= \gamma(\lambda) - z \end{aligned} \right\} \xrightarrow{\varepsilon,\beta \to 0} \left\{ \begin{aligned} t'^\beta &= 0 \\ y'^\beta &= 0 \\ z'^\beta &= \gamma(\lambda) - z \end{aligned} \right. , \tag{33}$$

which describes dynamics in the sticking state $v = \varepsilon u \xrightarrow{\varepsilon \to 0} 0$. This has equilibria on $\mathcal{B}(z)$ as defined in (22), and implies the following:

Proposition 2 *Relaxation dynamics in the static mode. On $u = 0$ the system (31) possesses locally invariant manifolds $\mathcal{C}^{\beta}_{static}$ that lie $\mathsf{O}(\beta)$ close to and diffeomorphic to the three-dimensional manifold $\mathcal{C}^{0}_{static} = \left\{ (t, y, z, \lambda) : \mathbb{R}^3 \times [-1, +1] : z = \gamma(\lambda) \right\}$.*

Proof On $u = 0$, the three-dimensional manifold $\mathcal{C}^{0}_{static}$ is the set of equilibria of the limiting system (33) with $\beta = 0$ and $\varepsilon = 0$. These are normally hyperbolic since $\partial z'^{\beta} / \partial z = -1$, thus by Fenichel's theorem the system (30) has a locally invariant manifold $\mathcal{C}^{\beta}_{static}$ that lies $\mathsf{O}(\beta)$ close to and diffeomorphic to $\mathcal{C}^{0}_{static}$.

Inside this relaxed state we have dynamics on the fast timescale $\tau_\varepsilon = t/\varepsilon$, the derivative with respect to which we denote x'^{ε} for any variable x, giving

$$
\left.
\begin{aligned}
t'^{\varepsilon} &= \varepsilon \\
y'^{\varepsilon} &= \varepsilon^2 u \\
u'^{\varepsilon} &= \ddot{q} - ky - c\varepsilon u - N\Lambda_1(u)(1 + \rho z) \\
\beta z'^{\varepsilon} &= (\Gamma_1(u) - z)\varepsilon
\end{aligned}
\right\}
\xrightarrow{\varepsilon \to 0}
\left\{
\begin{aligned}
t'^{\varepsilon} &= 0 \\
y'^{\varepsilon} &= 0 \\
u'^{\varepsilon} &= \ddot{q} - ky - N\Lambda_1(u)(1 + \rho z) \\
z'^{\varepsilon} &= 0
\end{aligned}
\right. .
$$
(34)

From this we have:

Proposition 3 *Sticking manifolds: In the system (26) there exist invariant manifolds $\mathcal{B}^{\varepsilon}(z)$ in the ε-neighbourhood of $\mathcal{B}(z)$ as given by (22).*

Proof The equilibria of the limiting ($\varepsilon = 0$) fast subsystem (34) are hyperbolic in a region satisfying $\Gamma_1(u) > 0$, since the system is one-dimensional and has eigenvalue

$$
\frac{\partial u'^{\varepsilon}}{\partial u} = -N(1 + \rho z_0)\frac{d\Lambda_1(u)}{du} = -N(1 + \rho z)\Gamma_1(u) < 0 \ ,
$$

for $z > -1/\rho$, the quantity z being constant in the system (34). Thus by Fenichel's theorem there exist locally invariant manifolds $\mathcal{B}^{\varepsilon}(z)$ that lie within $\mathsf{O}(\varepsilon)$ of and diffeomorphic to $\mathcal{B}(z)$.

The condition $\Gamma_s(u) > 0$ is clearly important, and means that these manifolds are only invariant for u sufficiently far away from ± 1.

To show that the dynamics on $\mathcal{B}^{\varepsilon}(z)$ is topologically equivalent to the sticking dynamics (24) we must replace the variable u.

Proposition 4 *Sticking dynamics: The dynamics on the manifolds $\mathcal{B}^{\varepsilon}(z)$ is topologically equivalent to the sticking dynamics of (24).*

Proof We define a new variable $L = \Lambda_1(u)$. Since $\Lambda_1(u)$ by (5) is single-valued, continuous and monotonic, it has an inverse which we write as $u = u(L)$. The variation of L is found using (10), and gives the dynamics of the variables $\{t, y, L, z\}$ as

$$
\left.
\begin{aligned}
\dot{t} &= 1 \\
\dot{y} &= \varepsilon u(L) \\
\frac{\varepsilon}{\tilde{\Gamma}^p(L)}\dot{L} &= \ddot{q} - ky - \varepsilon c u(L) - NL(1 + \rho z) \\
\beta \dot{z} &= \tilde{\Gamma}(L) - z
\end{aligned}
\right\}
\xrightarrow{\varepsilon \to 0}
\left\{
\begin{aligned}
\dot{t} &= 1 \\
\dot{y} &= 0 \\
0 &= \ddot{q} - ky - N\lambda(1 + \rho z) \\
\beta \dot{z} &= \gamma(\lambda) - z
\end{aligned}
\right.
$$
(35)

on the slow t timescale, and

$$\left.\begin{array}{l} t' = \frac{\varepsilon}{\tilde{\Gamma}(L)} \\ y' = \varepsilon^2 u(L)/\tilde{\Gamma}(L) \\ L' = \ddot{q} - ky - \varepsilon cu(L) - NL\left(1 + \rho z\right) \\ \beta z' = (\tilde{\Gamma}(L) - z)\varepsilon/\tilde{\Gamma}(L) \end{array}\right\} \xrightarrow{\varepsilon \to 0} \left\{\begin{array}{l} t' = 0 \\ y' = 0 \\ \lambda' = \ddot{q} - ky - N\lambda\left(1 + \rho z\right) \\ z' = 0 \end{array}\right. \quad (36)$$

on the fast t/ε timescale, denoting the relevant derivative by a prime. The limiting systems are equivalent to those of the nonsmooth system (24) and (21) respectively.

(Similar methods for biological models regulated by monotonic 'Hill' switching functions can be found in [40], but here we have certain added complexities, particularly non-monotonic switching due to Γ and hysteresis due to z).

These results are sufficient to show that simulations of systems of the form (26), a smooth approximation of the discontinuous system (25), lie ε-close to those of the discontinuous system described in section 6, and moreover can be studied using further methods of singular perturbation theory with respect to the singular perturbation parameters β and ε. For example, from the work of Eckhaus [21] one expects the flow to take $\mathsf{O}\left(1\right)$ time to travel along the slow manifold $\mathcal{B}(z)$, until reaching a turning point where normal hyperbolicity is lost, then jump off to rejoin the fast flow. In the much studied van der Pol system this jumping off takes place within a time $\mathsf{O}\left(\varepsilon^{1/3}\right)$ and within a distance $\mathsf{O}\left(\varepsilon^{2/3}\right)$ of the turning point, while in the system above the result depends on $\ddot{q}$ and the calculations are lengthy, but make an interesting subject for future work.

The final consideration is how the flow transitions between the $|v| > \varepsilon$ dynamics of Proposition 1 and the $|v| < \varepsilon$ dynamics of Propositions 2-4. The transition between the slow dynamics (27) that reigns in the region $|v| > \varepsilon$, and the fast dynamics (34) that dominates the region $|v| < \varepsilon$ by Proposition 3, is transversal if $\dot{v} \neq 0$. This therefore holds away from the tangencies where $\dot{v} = 0$ on $|v| = \varepsilon$, which are the points where the slow manifold $\mathcal{B}(z)$ meet the boundary layer $|v| = \pm\varepsilon$, and which form the boundaries of the linear sticking region as described in section 5. The result of these transitions are seen in stick-slip dynamics in the following section.

8 Smoothed-out simulation, $\varepsilon > 0$

For the sake of simulation we use the smoothed-out form of the system (25) given by (26), in terms of functions $\Lambda_\varepsilon(v)$ and $\Gamma_\varepsilon(\Lambda)$ consistent with (6) and (7). For the function $\Lambda_\varepsilon(v)$ which smooths out the discontinuity in $\text{sign}(v)$, any monotonic function $\Lambda_\varepsilon(v)$ that satisfies $\Lambda_\varepsilon(v) \to \Lambda(v)$ as $\varepsilon \to 0$ should suffice. For all simulations made here we take $\Lambda_\varepsilon(v) = \frac{v/\varepsilon}{\sqrt{1+(v/\varepsilon)^2}}$ and $\Gamma_\varepsilon(v) = \frac{1}{1+(v/\varepsilon)^2}$, but remark that alternatives such as $\Lambda_\varepsilon(v) = \text{Erf}(v/\varepsilon)$ or $\Lambda_\varepsilon(v) = \tanh v/\varepsilon$ reveal similar behaviour to what follows. The resulting smoothly-varying system will be stiff near $|v| \lesssim \varepsilon$ for small ε.

We apply a driving oscillation $\ddot{q}(t) = -\sigma \sin \omega t$, so the model consists of three sets of parameters: ρ, ε, and β for the friction model; k, c and N, for the bouncer; ω and σ for the shaker. Experimental, numerical, and analytical studies of similar

oscillator models can be found in [23, 37, 28, 30, 48, 15], but in analytical consider-
ations these predominantly consider $\rho = 0$ only.

The shading in figure 8 shows linear and nonlinear sticking regions. One period
of a stick-slip oscillation is shown. Once per period the trajectory sticks for a time
interval $\delta t \approx \pi/2$, and once per period it crosses directly between right-slip and
left-slip at around $t \approx -3\pi/4$. The relaxation time β is sufficiently fast for static
friction to be observed as of spikes in the friction characteristic in figure 8(top-left).
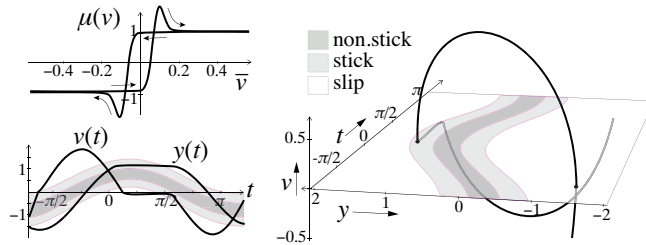

Fig. 8 Simulation of (26) with $\varepsilon = 0.1$, $\beta = 0.1$, $\lambda_s = 2/3$ ($\rho = 3$), $k = 3.1$, $c = 0.1$, $N = 1$,
$\sigma = 2.4$, $\omega = 1$. Top left: the friction characteristic $\mu(v)$ plotted along the simulated trajectory,
as a function of the 'compliant speed' $\bar{v} = v - \varepsilon y$ introduced in figure 7. Right: a trajectory of
the periodic orbit. Bottom left: a plot of the y and v variables. Shading indicates the regions of
linear sticking (dark grey) and nonlinear sticking (light grey) from (18)-(19). A stick-slip oscillation
is seen, with sticking occurring in the nonlinear region. This and all subsequent simulations are
performed in Mathematica®.

As we take successively smaller ε, the friction characteristic (top-left in fig-
ure 8) tends towards the set-valued system in figure 7(ii); one such simulation is
shown in figure 9(i), comparing favourably with figure 1(iv), and providing a sim-
ple smoothing of figure 7(ii). If we take the relaxation time β to be slower than the
smoothing parameter ε then, during direct transition from left to rightward slip,
there will be insufficient time spent near $v = 0$ for static friction to be exhibited,
causing the spike in the upper branch of the friction characteristic to shrink as in
figure 9(ii). During sticking, however, the system spends sufficient time near $v = 0$
for the static friction coefficient to reach its peak, so the spike in the lower branch
at the transition from stick to left-slip is unaffected between (i) and (ii) of figure 9.
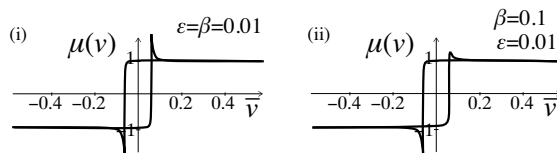

Fig. 9 The friction characteristic as ε is taken to zero. All value are as in figure 8, except: in (i)
$\varepsilon = \beta = 0.01$, in (ii) $\varepsilon = 0.01$, $\beta = 0.1$.

Note that the trajectory in figure 8 sticks (evolves along $v = 0$) in the *nonlinear*
sticking region (light grey), which only exists if we include the nonlinear depen-

dence of μ on Λ, i.e. when $\rho \neq 0$. The kinetic friction model with $\rho = 0$ would only stick in the linear region (dark grey), so upon setting $\rho = 0$ we obtain an oscillation with left and rightward slip only, as in figure 10.

It is important to note here that the switching on or off of nonlinear terms by ρ crucially changes the *global* dynamics — a cycle with stick in figure 8 but without stick in figure 10.
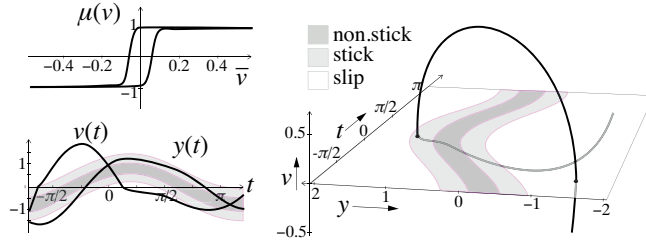

Fig. 10 Simulation corresponding to figure 8 but with $\rho = 0$, showing an oscillation with left and rightward slip only, which pierces the nonlinear sticking region (light grey) without sticking.

In [34] it was predicted that nonlinear sticking of the kind seen in figure 8 was robust to random perturbations only up to a certain magnitude (this might include environmental noise or roughness of the contact patch, though the only specific source of perturbations studied in detail so far has been that of external white noise [35]). The results holds for perturbations κ on the order of the smoothing parameter ε, when both are small. We introduce such perturbations to our simulation by applying a random perturbation of size κ to the state $\{y, v\}$ after every $1/500^{th}$ of a period (similar dynamics is obtained if perturbations are also made in z). The simulation in figure 11 shows that nonlinear sticking persists for perturbations of size $\kappa = \varepsilon/5$, but is destroyed in figure 12 by perturbations of size $\kappa = 5\varepsilon$. Note that
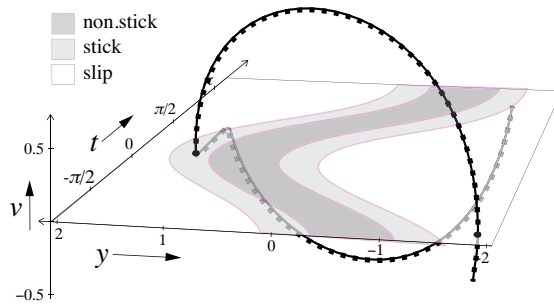

Fig. 11 Simulation corresponding to figure 8 showing a stick-slip oscillation subject to no perturbation (full curve) or to small noise of size κ (dotted curve), obtained with $5\kappa = \varepsilon = \beta = 0.001$, $\lambda_s = 2/3$ ($\rho = 3$), $k = 3.1$, $c = 0.1$, $N = 1$, $\sigma = 2.4$, $\omega = 1$.

κ is small enough that the noisy and noise-less trajectories closely coincide almost everywhere, the perturbations only having a significant effect near $v = 0$, where they eliminate nonlinear sticking in the latter case, for small noise the nonlinear

terms, and the difference between static and kinetic friction they produce, persist under what are effectively two different perturbations: the small added noise, and the smoothing of the discontinuity (figure 11). With sufficient noise the system behaves as if $\rho = 0$, and hence neglects static friction (figure 12), removing the segment of sticking.
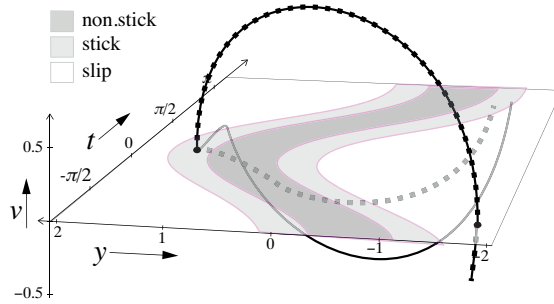

Fig. 12 Simulation corresponding to figure 8 showing a stick-slip oscillation subject to no perturbation (full curve), and the effect on this trajectory of small noise of size κ (dotted curve), obtained with $\kappa/5 = \varepsilon = \beta = 0.001$, $\lambda_s = 2/3$ ($\rho = 3$), $k = 3.1$, $c = 0.1$, $N = 1$, $\sigma = 2.4$, $\omega = 1$.

Lastly we show in figure 13 the friction characteristics for these two simulations, confirming for $\kappa < \varepsilon$ that the peaks consistent with static friction still appear in the presence of noise (dotted curve), but for $\kappa > \varepsilon$ the perturbations are large enough to cause the trajectory to miss the peaks that constitute static friction. Very little compliance is visible here because ε is small.
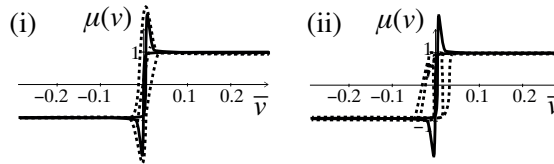

Fig. 13 Friction characteristics for the simulations in figure 11 and figure 12 respectively, constituting (i) small noise and (ii) large noise. The full curve shows the unperturbed simulation. The dotted curve shows the perturbed simulation, which exhibits the static friction peaks in (i), but misses them in (ii).

A similar two-dimensional problem without driving studied in [34,35] showed that nonlinear sticking can mean the difference between decay to a steady state (with $\rho = 0$), and trapping into a stick-slip oscillation (with $\rho \neq 0$). Moreover in [35] it was shown in a stochastic setting that sticking modes can be interpreted as potential wells, escapable under sufficient perturbation due to noise.

9 Closing remarks and friction-inspired models

In effect, the standard theory of piecewise-smooth dynamical systems amounts to assuming the true system is a regular perturbation (1) of a discontinuous system

(see [25] and also [2]). Discontinuous functions as approximations are, however, more commonly encountered in *singular* perturbations, which may take different analytic forms on disjoint domains, and therefore exhibit discontinuities in the transition between regions (in this case at $v = 0$)

Other than the model considered in section 2, there are many specific physical bases upon which one might build an argument for the kind of nonlinear switching terms considered here. While it is to be hoped that these models can be improved by detailed comparison with experiment, improvements in our general mathematical intuition are helpful in navigating the multitude of possible physical considerations. Early theories modelled friction by considering interaction of surface features such as asperities [4, 9, 16, 42, 43], but static friction and stick-slip are observed even in asperity free and atomically smooth interfaces [38, 32], and dissipation of energy via phonons seems to play a crucial role [38, 53, 14]. Other models attribute friction to a drag effect due to energy loss through phonon generation [3, 10, 46], or electronic drag not due to van der Waals forces but to currents in the electron cloud [44]. In seeking greater insight, attention turns to microscopic effects such as atom-scale deformations [54], macro-microscale stress interactions during relaxation [47], or third body effects of adsorbed molecules acting as pins [29], and building from these to reproduce macro-scale behaviour is where discontinuous models may help. The model (5) provides a mathematical framework by which such small-scale structure can be captured in a discontinuity, and using a toy model based on its key properties, we showed how this leads naturally to friction characteristics such as static friction and hysteresis.

One enduring attraction of Coulomb's kinetic friction model is that it expresses friction with only a single parameter: a coefficient giving a fixed proportionality to the normal load, (and in mathematical analysis even this parameter can be scaled to unity). Generalisations of the model that replace the discontinuity (figure 1(i)) with a smooth nonlinear function (e.g. figure 1(iv)) cause the list of parameters to grow quickly. Models of a dynamically evolving friction force are traceable from Dahl [16] through various developments to, for example, the LuGre model [8, 4, 42] where a friction force $F = k_s z + c_s \dot{z} + cv$ evolves according to the deflection z of bristles on the surface, with stiffness k_s and damping c_s, including a viscous friction coefficient c, and Stribeck velocity v_{str} below which speed dependence is seen; bristle models capture the key effects of friction and yield a smooth force law, and have inspired many variations on the model, usually bringing with them more coefficients connected with nonlinearities, giving dependence on acceleration or forming alternative models of asperities. For example in [55] it was proposed to switch the contact force between accelerative, decelerative, and static modes, requiring several quantifiers of effects including compliance or friction memory and hysteresis, Stribeck velocity dependence, dwell times in stick-slip transition, and static friction.

The interesting and most general open problem is then to relate the nonlinearity that enters via the second term of a switching model of the form $\mu(v) = \Lambda(v) + L(v)\Gamma(v)$ to specific applications. The addition of nonlinear terms via the function Γ is an obvious generalization of Filippov's method [25] introduced in [34], which furthermore gains an interpretation in terms of potential wells in a stochastic framework discussed in [35]. The key property is that the nonlinear terms are only of significant size at or near the discontinuity, introduced by functions of the form (7). In typical applications these nonlinearities might be associated with

an energy cost involved in the switching process (e.g. noise, adhesion, or adverse heating), as one example. The choice $L = \Lambda$ made in (5) was a simple example that, as shown, is able to account for static friction, and one may seek to derive a more precise form from any of the underlying physical processes mentioned above.

The practical problems of stick-slip (e.g. squealing brakes) and static friction (jolt when released from stick) remain a source of wear and instability in mechanical engineering, and moreover with modern applications revealing stick-slip dynamics on scales ranging from earthquake dynamics to atomic force microscopy, the story of friction is far from its end. The interest in such dynamics also goes beyond friction, since much of our mathematical modeling of social, biological, and other neoteric physical or engineering dynamical systems, draws inspiration from familiar notions in classical mechanics, among them relays in electronic circuits, biochemical switching in neural pathways or cell growth, and decision making in social behaviour. The mathematical description of friction therefore has implications for our understanding of interaction dynamics in the broader sciences. The results we derive here can be applied to switching dynamics in all such systems.

A Switching asymptotics

The main contributions to the integral (3) come from the maxima of the envelope $a(k)$. There may be many such maxima, but near each we obtain expressions of the following form. We expand the phase $\theta(k)$ as a Taylor series, and with a little manipulation we approximate the integral as an envelope which is gaussian $a(k) \approx e^{-k^2/2}$ or gaussian-like (e.g. $a(k) \approx 1/(1+k^2)$), with a linear phase $\theta(k) \approx \rho k$ for constant ρ. Taking for example $a(k) = e^{-k^2/2}$ we have

$$
\begin{aligned}
\mu(v) &= \mathrm{Re}\left[\mathrm{Erf}\left(\frac{v/\varepsilon - i\rho}{\sqrt{2}}\right)\right] \\
&\sim \mathrm{sign}(v) - \sqrt{\frac{2}{\pi}} e^{(\rho^2 - v^2/\varepsilon^2)/2} \, \mathrm{Re}\left[e^{i\rho v/\varepsilon} \sum_{n,m=0}^{\infty} \frac{(i\rho)^m C_{nm}}{(v/\varepsilon)^{2n+1+m}}\right] \\
&\sim \mathrm{sign}(v) \times \left\{1 - \sqrt{\frac{2}{\pi}} \frac{e^{(\rho^2 - v^2/\varepsilon^2)/2} \cos(\rho v/\varepsilon)}{|v|/\varepsilon} + ...\right\}.
\end{aligned}
\tag{37}
$$

The first line denotes the real part of the standard error integral [1] denoted Erf, the second (with coefficients $C_{nm} = \frac{(-1)^n (2n-1)!!(2n+1)!}{(2n+1-m)!m!}$) follows from its asymptotic approximation for large argument and $|v|/\varepsilon \gg \rho$, whose leading order terms are shown in (37). The v/ε limit of the integral introduces a cut-off similar to Gibbs phenomenon in Fourier series or ringing in signal control [27]. Taking $a(k)$ to be any of $e^{-k^2/2}$, $1/(1+k^2)$ or $\mathrm{sech}^2(k)$, even when introducing more complex oscillations by replacing $\cos\theta(k)$ with, say, $\cos(\rho_1 k)\cos(\rho_2 k)$ or $\cos(\rho_1 k)\sin(\rho_2 k)/k$, all yield the same asymptotic form (2). These all tend towards a curve like figure 2(ii) in the limit $\varepsilon \to 0$, which has peak values $\mu = \pm\mu_s$ which are ε-independent and therefore remain clearly defined in the limit $\varepsilon \to 0$. In the example (37) the peak has height $\mu_s \sim 1 + \sqrt{\frac{2}{\pi}} \frac{4\rho^3}{\pi^2} e^{-\pi^2/8\rho^2}$ and lies at $v \sim \pm\pi\varepsilon/2\rho$.

To obtain (5) from (4) we can then define a continuous monotonic approximation of the sign function, a suitable and convenient choice being

$$
\Lambda_\varepsilon(v) = \frac{v/\varepsilon}{\sqrt{1 + (v/\varepsilon)^2}} = \mathrm{sign}(v) - \sum_{n=1}^{\infty} \frac{b_n}{(iv/\varepsilon)^{2n}},
\tag{38}
$$

which satisfies (6), with coefficients $b_n = \frac{\text{sign}(v)}{(2n)!} \prod_{m=1}^{n} (2m-1)^2$. Using (38) to replace the sign function in (4), we obtain

$$\mu(v) \sim \Lambda_\varepsilon(v) + \sum_{n=1}^{\infty} \left\{ i^{2n} b_n + c_n q(v/\varepsilon) \right\} (\varepsilon/v)^{2n}$$

$$:= \Lambda_\varepsilon(v) + \rho L_\varepsilon(v) \Gamma_\varepsilon(v) , \tag{39}$$

the second line being found by substituting v/ε with its inverse $v/\varepsilon = \Lambda_\varepsilon / \sqrt{1 - \Lambda_\varepsilon^2}$. Based on the qualitative form of (37) we approximate $L_\varepsilon(v)$ in (39) as $L_\varepsilon(v) = \Lambda_\varepsilon(v)$ for the sake of the friction model in (5). The constant ρ controls the peak height μ_s of the function $\mu(v)$, the precise relation depending on the functional form of μ. The result (39) is expressed in terms of the function $\Gamma_\varepsilon(v) = 1 - \Lambda_\varepsilon^2(v)$ which satisfies (7), and

$$L_\varepsilon(v) = \frac{1}{\rho} \sum_{n=1}^{\infty} \frac{i^{2n} b_n + c_n q(v/\varepsilon)}{\Lambda_\varepsilon^{2n}(v)} \left(1 - \Lambda_\varepsilon^2(v) \right)^{n-1}$$

$$= \frac{c_1 q(v/\varepsilon) - b_1}{\rho \Lambda_\varepsilon^2(v)} + \mathsf{O}\left(1 - \Lambda_\varepsilon^2(v) \right) , \tag{40}$$

where ρ serves as a normalisation constant at $v = 0$. The finiteness of $L_\varepsilon(v)$ at $v = 0$ follows from that of μ. In (40) we separate the leading order term in $L_\varepsilon(v)$ from those of order $1 - \Lambda_\varepsilon^2(v)$, which vanish as $|v|/\varepsilon \to \infty$.

The asymptotic form (37) lends some interpretation to the features of the friction curves in figure 2. The $\text{sign}(v)$ term is the dominant contribution to the integral, arising from wavenumbers associated with lower energies and thus independent of the speed-dependent high energy cut-off at wavenumber $k = v/\varepsilon$, and this clearly corresponds to the kinetic friction component figure 1(i). At small v the cut-off becomes important, creating decay away from the steady value $|\mu| \approx 1$ towards $\mu \approx 0$, plus an oscillation dominated by wavenumbers near $k_* = v/\varepsilon$ that results in peaks at $\pm \mu_s$; in the Gaussian model these occur at $v = \pm v_s := \pi \varepsilon / 2\rho$. The peak amplitude μ_s is ε independent (since v_s/ε can everywhere be replaced by $\pi/2\rho$), so the peaks remain at the same height as $\varepsilon \to 0$ as shown in figure 2(ii), reproducing the static friction component of figure 1(ii). For $\rho = 0$ there are no peaks, while for larger ρ there appear multiple peaks and dips at small but non-zero speeds (not shown); these dips in the friction force may or may not have physical application.

The peak seen in figure 2 is just the first of a sequence of oscillations that grow as we take ρ larger (i.e. a faster oscillating integrand), and they need not (though they do in this case) grow so rapidly in amplitude with ρ. Such oscillations may be of interest for modeling elsewhere, and can be dealt with using similar methods to those we introduce, but we limit this paper to investigating the application of a single peak model to a simple friction problem.

B Perturbation to $\beta > 0$ and $\varepsilon > 0$

Consider the full discontinuous system (25) for small $\beta > 0$, in terms of variables $\{y, v, z\}$ and the functions $\Lambda(v)$, $\Gamma(v)$, from (6)-(7). On $v = 0$ the values $\Lambda(0)$ and $\Gamma(0)$ shall be replaced by dummy variables λ and $\gamma(\lambda)$ according to (9).

Proposition 5 *For* $\max[|\ddot{q}(t)|] \leq N\mu_s$ *there exists a strip of periodic orbits with fixed*

$$\{y(t), v(t), z(t)\} = \{y_0, 0, \gamma(\zeta)\}$$

satisfying $|y_0| \leq (N\mu_s - \max[\ddot{q}(t)]) / k$ *and with* ζ *any solution of*

$$0 = \ddot{q} - k y_0 - N\zeta \left(1 + \rho \gamma(\zeta) \right) : \quad |\gamma(\zeta)| \leq 1 .$$

If $\lambda_s > 1$ *with* λ_s *defined by (16), these periodic orbits are all attracting, if* $\lambda_s < 1$ *those with* $|\zeta| < \lambda_s$ *are attracting and those with* $\lambda_s < |\zeta| \leq 1$ *are of saddle-type.*

Proof A solution of (25) with fixed $\{y, v, z\}$ must clearly have $v(t) = 0$ and $z(t) = \Gamma(v)$, which implies a sticking trajectory. Therefore we use the sticking variables (9). By (19) sticking trajectories must satisfy $\ddot{q}(t) - N\mu_s \leq ky(t) \leq \ddot{q}(t) + N\mu_s$, and for fixed values $y(t) = y_0$ to exist it is sufficient to have $\max[\ddot{q}(t)] - N\mu_s \leq ky_0 \leq -\max[\ddot{q}(t)] + N\mu_s$, which has solutions for y_0 only if $\max[\ddot{q}(t)] \leq N\mu_s$. The eigenvalue along the ζ-direction is $\frac{\partial \dot{z}}{\partial z} = -1$ by (25) and therefore attracting, and note that y is stationary in the sticking mode by (21) and (24). Finally, sticking solutions satisfy (24) and therefore lie in the surface $\mathcal{B}(z)$ defined in (22), obeying $\lambda(t) = \zeta$ for some ζ, which implies $0 = \ddot{q} - ky_0 - N\zeta(1 + \rho\gamma(\zeta))$. Such a fixed point is attracting if $\frac{\partial \lambda'}{\partial \lambda} < 0$ and since $\frac{\partial \lambda'}{\partial \lambda} = -N(1 + \rho\gamma(\zeta))$ substituting $\lambda = \lambda_s$ and re-arranging gives $|\zeta| < \lambda_s$, which applies if $\lambda_s < 1$, and otherwise $|s| < 1$ if $\lambda_s \geq 1$, in short $|\zeta| < \max[1, \lambda_s]$.

As a simple corollary, when $N\mu_s = |\ddot{q}|$ there is only one sticking periodic orbit, given by $\{y(t), v(t), z(t)\} = \{0, 0, 0\}$, which passes through at least one point on the sticking boundary, thus undergoing some form of *sliding bifurcation*. For example if we take $\ddot{q}(t) = -\sigma \sin(\omega t)$ then the sticking boundary and the periodic orbit contact tangentially at $t = \frac{\pi}{2\omega}$ where the right-slipping speed vanishes, i.e. $\lim_{\delta \to 0} \dot{v}|_{v=+\delta} = 0$ with $\delta \geq 0$, and at $t = \frac{3\pi}{2\omega}$ where the right-slipping speed vanishes, i.e. $\lim_{\delta \to 0} \dot{v}|_{v=-\delta} = 0$ with $\delta \geq 0$.

When $N\mu_s < |\ddot{q}|$ there no longer exist pure sticking periodic orbits (i.e. purely within $v = 0$), but one expects, since the system is dissipative, there to exist at least one attractor. Typical behaviour of piecewise-smooth systems suggests that these will take the form of stick-slip periodic orbits for parameters close to $N\mu_s = |\ddot{q}|$, undergoing brief intervals of sticking between intervals of right and/or left slipping motion, though a complete study is beyond our scope here. Stick-slip orbits were found in the case of the undamped $c = 0$ and non-hysteretic $\beta = 0$ oscillator, and for a sinusoidal forcing $\ddot{q}$, in [28,37]. Crucially these and other previous works that use Filippov-type solutions assume linear sticking, i.e. $\rho = 0$. Some numerical simulations and experiments are given in [15,55], showing periodic, quasi-periodic, and irregular motions, suggesting that further in-depth analytical studies are an interesting subject for future work; note that the analysis in [55] introduces hysteresis and static friction using multiple switching laws, instead of nonlinear sticking as introduced here, and various multi-period orbits are identified in numerical and experimental data. In simulations similar to those in section 8 but not shown here, periodic left-right slip and periodic stick-slip oscillations are found at a wide range of parameters.

References

1. M. Abramowitz and I. Stegun. *Handbook of Mathematical Functions*. Dover, 1964.
2. M. A. Aizerman and E. S. Pyatnitskii. Fundamentals of the theory of discontinuous systems I,II. *Automation and Remote Control*, 35:1066–79, 1242–92, 1974.
3. A. Akay. Acoustics of friction. *J. Acoust. Soc. Am.*, 111(4):1525–1548, 2002.
4. F. Al-Bender, V. Lampaert, and J. Swevers. A novel generic model at asperity level for dry friction force dynamics. *Tribology Letters*, 16(1):81–93, 2004.
5. G. Bachar, E. Segev, O. Shtempluck, E. Buks, and S. W. Shaw. Noise induced intermittency in a superconducting microwave resonator. *EPL*, 89(1):17003, 2010.
6. J. Bastien, and G. Michon, and L. Manin, and R. Dufour. An analysis of the modified Dahl and Masing models: Application to a belt tensioner. *Journal of Sound and Vibration*, 302(4-5)841-864 (2007).
7. M. V. Berry. Stokes' phenomenon; smoothing a Victorian discontinuity. *Publ. Math. of the Institut des Hautes Études scientifique*, 68:211–221, 1989.
8. P-A Bliman and M Sorine. Easy-to-use realistic dry friction models for automatic control. In *Proceedings of 3rd European Control Conference*, pages 3788–3794, 1995.
9. F P Bowden and D Tabor. The friction and lubrication of solids, 1964.
10. O. M. Braun, T. Dauxois, and M. Peyrard. Friction in a thin commensurate contact. *Phys. Rev. B*, 56(8):4987–4995, 1997.
11. B. Brogliato. *Nonsmooth mechanics – models, dynamics and control.* Springer-Verlag (New York), 1999.
12. B. Brogliato and V. Acary. *Numerical methods for nonsmooth dynamical systems.* Springer Verlag, Lecture Notes in Applied and Computational Mechanics (35) 2008.
13. C. Studer *Numerics of Unilateral Contacts and Friction.* Springer Verlag, Lecture Notes in Applied and Computational Mechanics (47) 2009.

14. M. Cieplak, E.D. Smith, and M.O. Robbins. Molecular origins of friction: The force on adsorbed layers. *Science*, 265(5176):1209– 1212, 1994.
15. G. Csern'ak and G. Stépán. On the periodic response of a harmonically excited dry friction oscillator. *Journal of Sound and Vibration*, 295:649–658, 2006.
16. P. R. Dahl. A solid friction model. *TOR-158(3107-18), The Aerospace Corporation, El Segundo, CA*, 1968.
17. B. Derjaguin. Molekulartheorie der äusseren Reibung. *Zeitschrift für Physik*, 88(9-10):661– 675, 1934.
18. M. di Bernardo, C. J. Budd, A. R. Champneys, and P. Kowalczyk. *Piecewise-Smooth Dynamical Systems: Theory and Applications*. Springer, 2008.
19. L. Dieci and L. Lopez. A survey of numerical methods for IVPs of ODEs with discontinuous right-hand side. *Journal of Computational and Applied Mathematics*, 236(16):3967–3991, 2012.
20. R. B. Dingle. *Asymptotic Expansions: their derivation and interpretation*. Academic Press London, 1973.
21. W Eckhaus. Relaxation oscillations including a standard chase on French ducks. *Lect. Notes Math.*, 985:449–494, 1983.
22. C.P. Fall, E.S. Marland, J. M. Wagner, and J.J. Tyson. *Computational Cell Biology*. New York, Springer-Verlag, 2002.
23. B. Feeny and F.C. Moon. Chaos in a forced dry-friction oscillator: Experiments and numerical modelling. *J. Sound Vib.*, 170(3):303–323, 1994.
24. N. Fenichel. Geometric singular perturbation theory. *J. Differ. Equ.*, 31:53–98, 1979.
25. A. F. Filippov. *Differential Equations with Discontinuous Righthand Sides*. Kluwer Academic Publ. Dortrecht, 1988.
26. E. Gnecco, R. Bennewitz, T. Gyalog, Ch. Loppacher, M. Bammerlin, E. Meyer, and H.-J. Güntherodt. Velocity dependence of atomic friction. *PRL*, 84(6):1–4, 2000.
27. D. Gottlieb and Chi-Wang Shu. On the Gibbs phenomenon and its resolution. *SIAM Review*, 39(4):644–668, 1997.
28. M. Guardia, S. J. Hogan, and T. M. Seara. An analytical approach to codimension-2 sliding bifurcations in the dry friction oscillator. *SIAM J. Dynamical Systems*, 2010.
29. G. He, M. M. Muser, and M. O. Robbins. Adsorbed layers and the origin of static friction. *Science*, 284(5420):1650–1652, 1999.
30. N. Hinrichs, M. Oestreich, and K. Popp. On the modelling of friction oscillators. *J. Sound Vib.*, 216(3):435–459, 1998.
31. A.L. Hodgkin and A.F. Huxley. A quantitative description of membrane current and its application to conduction and excitation in nerve. *J Physiol.*, 117(4):500–544, 1952.
32. J.N. Israelachvili. *Fundamentals of Friction*, chapter Adhesion, Friction and Lubrication of Molecularly Smooth Surfaces. Kluwer, Dortrecht Edited by I.L. Singer and H.M. Pollock, 1992.
33. M. R. Jeffrey. Non-determinism in the limit of nonsmooth dynamics. *Physical Review Letters*, 106(25):254103, 2011.
34. M. R. Jeffrey. Hidden dynamics in models of discontinuity and switching. *Physica D*, 273-274:34–45, 2014.
35. M. R. Jeffrey and D. J. W. Simpson. Non-Filippov dynamics arising from the smoothing of nonsmooth systems, and its robustness to noise. *Nonlinear Dynamics*, 76(2):1395-1410, 2014.
36. C. K. R. T. Jones. *Geometric singular perturbation theory*, volume 1609 of *Lecture Notes in Math. pp. 44-120*. Springer-Verlag (New York), 1995.
37. P. Kowalczyk and P.T. Piiroinen. Two-parameter sliding bifurcations of periodic solutions in a dry-friction oscillator. *Physica D: Nonlinear Phenomena*, 237(8):1053 – 1073, 2008.
38. J. Krim. Friction at macroscopic and microscopic length scales. *Am. J. Phys.*, 70:890–897, 2002.
39. Yu. A. Kuznetsov, S. Rinaldi, and A. Gragnani. One-parameter bifurcations in planar Filippov systems. *Int. J. Bif. Chaos*, 13:2157–2188, 2003.
40. A. Machina, R. Edwards, and P. van den Dreissche. Singular dynamics in gene network models. *SIAM J. Dynamical Systems*, 12(1):95-125, 2013.
41. D. D. Novaes and M. R. Jeffrey. Hidden nonlinearities in nonsmooth flows, and their fate under smoothing *submitted* January 2015.
42. H Olsson, K J Astrom, C C de Wit, M Gafvert, and P Lischinsky. Friction models and friction compensation. *Eur. J. Control*, 4:176–195, 1998.

43. Persson, B. N. J. Albohr, U. O, Tartaglino, A. I. Volokitin, and E. Tosatti. On the nature of surface roughness with application to contact mechanics, sealing, rubber friction and adhesion. *J. Phys.: Condens. Matter*, 17:R1–R62, 2005.

44. B. N. J. Persson and Z. Y. Zhang. Theory of friction: Coulomb drag between two closely spaced solids. *Phys. Rev. B*, 57(12):7327– 7334, 1998.

45. P. T. Piiroinen and Yu. A. Kuznetsov. An event-driven method to simulate filippov systems with accurate computing of sliding motions. *ACM Transactions on Mathematical Software*, 34(3):13:1–13:24, 2008.

46. V. Popov. Phonon contribution to friction stress in an atomically flat contact of crystalline solids at low temperature. *Zeitschrift für Angewandte Mathematik und Mechanik*, 80(S1):65–68, 2000.

47. M. Radiguet, D. S. Kammer, P. Gillet, and J.-F. Molinari. Survival of heterogeneous stress distributions created by precursory slip at frictional interfaces. *PRL*, 111(164302):1–4, 2013.

48. S. W. Shaw. On the dynamics response of a system with dry friction. *J. Sound Vib.*, 108(2):305–325, 1986.

49. J-J. E. Slotine and W. Li. *Applied Nonlinear Control*. Prentice Hall, 1991.

50. G. G. Stokes. On the discontinuity of arbitrary constants which appear in divergent developments. *Trans Camb Phil Soc*, 10:106–128, 1864.

51. D. Tabor. Triobology - the last 25 years. a personal view. *Tribology International*, 28(1):7–10, 1995.

52. M. A. Teixeira and P. R. da Silva. Regularization and singular perturbation techniques for non-smooth systems. *Physica D*, 241(22):1948–55, 2012.

53. G.A. Tomlinson. A molecular theory of friction. *Philos. Mag.*, 7(7):905–939, 1929.

54. A. J. Weymouth, D. Meuer, P. Mutombo, T. Wutscher, M. Ondracek, P. Jelinek, and F. J. Giessibl. Atomic structure affects the directional dependence of friction. *PRL*, 111(126103):1–4, 2013.

55. J. Wojewoda, S. Andrzej, M. Wiercigroch, and T. Kapitaniak. Hysteretic effects of dry friction: modelling and experimental studies. *Phil. Trans. R. Soc. A*, 366:747–765, 2008.